

DEVELOPMENT OF REACTOR MODEL FOR RESIDUE HYDROCONVERSION PROCESS

A PROJECT REPORT

Submitted by

**Shekhar Jyoti Pathak
(R670215015)**

In partial fulfillment of the requirement for the award of the degree of

MASTER OF TECHNOLOGY
in
CHEMICAL ENGINEERING
with specialization in
PROCESS DESIGN ENGINEERING



**DEPARTMENT OF CHEMICAL ENGINEERING
COLLEGE OF ENGINEERING STUDIES
UNIVERSITY OF PETROLEUM & ENERGY STUDIES**

Bidholi campus, Energy Acres,
Dehradun-248007

APRIL – 2017

UNIVERSITY OF PETROLEUM & ENERGY STUDIES DEHRADUN

BONAFIDE CERTIFICATE

This is to certify that the thesis entitled “**DEVELOPMENT OF REACTOR MODEL FOR RESIDUE HYDROCONVERSION PROCESS**” submitted by **SHEKHAR JYOTI PATHAK (R670215015)**, to the University of Petroleum and Energy Studies, for the award of the degree of **MASTER OF TECHNOLOGY in Chemical Engineering with specialization in Process Design** is a bonafide record of project work carried out by him under our supervision. The results embodied in this project review report are based on literature and the research in IOCL R&D. This data is based on research carried out in IOCL R&D, and hence only IOCL reserves all rights to patent, publish and present the data.

Signature of the External Guide with date
SK Shabina
RM
Department RT -II
IOCL R&D
Faridabad-121007

Signature of the Internal Guide with date
Niteen Ramchandra Yeole
Assistant Professor
Department of Chemical Engineering
UPES
Dehradun - 248007

Signature of the Head of the Department
Date:

DECLARATION BY THE SCHOLAR

I hereby declare that this submission is my own and that, to the best of my knowledge and belief, it contains no material previously published or written by another person nor material which has been accepted for the award of any other Degree or Diploma of the University or other Institute of Higher learning, except where due acknowledgement has been made in the text.

Shekhar Jyoti Pathak

R670215015

ACKNOWLEDGEMENT

A lot of support from many individuals has gone into this project work and I would like to take this opportunity to extend a sincere thanks to all of them.

First and foremost, I would like to express a profound gratitude and regards to my mentor, **SK SHABINA, RM, IOCL (R&D)** for giving me this unique and interesting topic to work on. Her exemplary guidance, monitoring, utmost patience and enthusiasm have helped me at every step throughout.

I am highly indebted to **The Chemical Engineering Department, University of Petroleum and Energy Studies, Dehradun** for giving me this opportunity to pursue an internship and work on a live industrial problem at IOCL(R&D), FARIDABAD. In addition, I extend a sincere thanks to **Dr. I. ROY CHOUDHURY, SRM, IOCL (R&D)** for his timely advice and encouragement throughout my project duration.

A special gratitude to my internal guide **Niteen Ramchandra Yeole, Assistant Professor, Department of Chemical Engineering, UPES, Dehradun** who extended all his support possible for the completion of this project.

Then, I would like to express my profound thanks to **Dr. P Vijay**, Head of Chemical Engineering Department, for his support in doing this project.

A sincere thanks to all those people whose names I might have missed out, for their cooperation in every possible way that helped me complete this project successfully.

Lastly I would like to thank the Almighty and acknowledge the support extended by my parents without which my stay at **FARIDABAD** would not have been a peaceful one.

Dated: 15th, April, 2017
Place: Dehradun

(**SHEKHAR JYOTI PATHAK**)

ABSTRACT

The aim of this research work is to study the kinetics of various reactions involved in HYDROCONVERSION OF RESIDUE of crude oil by developing a kinetic model. The kinetic model is based on the lumping method. A preliminary kinetic analysis based on the conversion of the residue was performed. A simplified kinetic yield model was applied; where the feed and each product fraction are represented by different lumps (reactant or product of cracking). The model results are obtained by solving the system of equation using MATLAB software. The results are then compared with the theoretical data.

Keywords: Residue, catalytic hydrocracking, mathematical model, chemical kinetics.

TABLE OF CONTENTS

DECLARATION BY SCHOLAR

CERTIFICATE

ACKNOWLEDGEMENT i

ABSTRACT ii

TABLE OF CONTENTS iii

LIST OF TABLES v

LIST OF FIGURE vi

CHAPTER 1 1

INTRODUCTION..... 1

1.1 INTRODUCTION TO HYDROPROCESSING 1

1.2 IMPORTANCE OF HYDROPROCESSING 1

1.3 CLASSIFICATION OF HYDROPROCESSING 2

1.4 STEPS INVOLVED IN HYDROCRACKING 2

CHAPTER 2 3

LUMPING METHOD 4

2.1 LUMPING TECHNIQUE..... 4

2.1.1. Discrete lumping models 5

 2.1.2 Structure oriented lumping and single event models 6

CHAPTER 3 8

LITERATURE REVIEW ON KINETIC MODEL 8

3.1 CRITICALLY INVOLVED IN MODELLING FOR RESIDUE CONVERSION 8

3.2 VARIOUS MODELS EXISTING FOR RESIDUE CONVERSION..... 8

CHAPTER 4 19

DEVELOPMENT OF MODEL FOR HYDROCRACKING OF RESIDUE	19
4.1 MODEL ASSUMPTIONS	20
4.2 REACTION PATHWAY INVOLVED IN THE MODEL.....	20
4.3 REACTION EQUATIONS FOR THE REACTING COMPOUNDS	21
4.4 KINETIC EXPRESSION FOR EACH OF THE LUMPS.....	21
4.5 CODING IN MATLAB FOR THE KINETIC MODEL	24
CHAPTER 5	28
RESULT AND DISCUSSION.....	28
CHAPTER 6.....	31
CONCLUSION	31
REFERENCES	32

LIST OF TABLES

1.1	Operating conditions involved in hydrocracking process.....	03
2.1	Rate constants for the hydrocracking of AR	06
3.1	Reactions of the models	10
3.2	Kinetic parameters for hydrocracking of vacuum residue.....	11
3.3	Kinetic parameters obtained from Model 10.....	12
3.4	Yields of VR hydrocracking	13
3.5	Comparison of data (Eduard and,Juma ,2014).....	17
4.1	Values of different stoichiometric coefficients	22
4.2	Rate constants at operating temperature of 420 and 430°C	23
4.3	Molecular weights and densities of the lumps.....	24
5.1	Data obtained for the lumps at 420°C.....	28
5.2	Data obtained for the lumps at 430°C	28

LIST OF FIGURES

1.1	Classification of hydroprocessing	02
2.1	Classification of lumping method	04
2.2	Reaction mechanism	05
3.1	Reaction pathways for model 1 (a) and model 10 (b).....	09
3.2	Reaction pathways.....	14
3.3	Comparison of the data.....	16
4.1	Kinetic scheme of the hydrocracking of residue.....	20
4.2	Comparison of the model data with experimental data 430°C.....	29
4.3	Comparison of the model data with experimental data at 420°C.....	30

CHAPTER 1

INTRODUCTION

The oil refinery, in the same way as other manufacturing industries must be progressively adjusted to real market needs. The implementation of newly developed technologies and modern innovations are very important in refineries for producing valuable products. So Present oil refinery scenario is focusing on the upgradation of the heavy oil into better quality distillate products.

The market needs for upgraded lighter products from the refinery is increasing every day. Petroleum industry is concentrating on the recovery of each valuable lighter fractions from each and every drop of oil applying modern technology. So refining technologies that produces low boiling products from the heavier crude fractions are of great importance to this industry to fulfill the market demand.

1.1 Introduction to Hydroprocessing

Hydroprocessing can be defined as a secondary process which includes the reactions of different heavy oil fractions with hydrogen as a part of oil refining in the refineries to produce better quality products. The hydroprocessing technology is of great importance in the refineries. It comes under the secondary processing carried out in the refinery for the heavier crude fractions.

1.2 Importance of hydroprocessing

1. Environmental standards: The environmental standards associated to emissions from fuels are getting stricter. It is a difficult task for the refiners to meet the strict standards that concern mainly sulfur, nitrogen, aromatics, oxygenates etc. present in the petroleum fractions.
2. Product properties: Product properties such as cetane number and smoke point can be improved by means of hydroprocessing.
3. Catalyst protection: Many catalysts are peculiarly sensitive to feed contaminants which have the ability to cause temporary or permanent catalyst deactivation. Some of the sensitive units in a refinery that require that safeguards are catalytic reformer, isomerization unit etc.

4. Optimizing product yields: Hydroprocessing deals with converting heavy oil fractions into low boiling and higher important products such as naphtha. Refiners can make rapid economic gains by optimizing product stream.

1.3 Classification of hydroprocessing

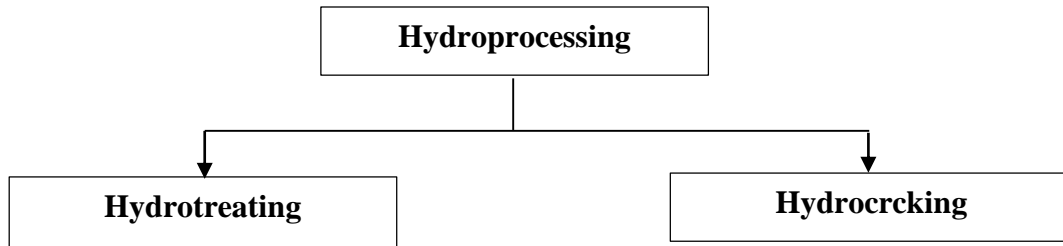


Figure 1: Classification of hydroprocessing

Hydrotreating –The basic purpose of hydrotreating process is to remove the contaminants such as sulfur, nitrogen, oxygen bearing compounds, metals, aromatics etc. from the heavy crude fractions. Such contaminants are undesirable in the petroleum products based on performance and environmental standards. Hydrotreating process removes the contaminants and saturate olefins and aromatics to upgrade the oil fractions as well as to produce clean products to meet the market demand.

Hydrocracking – It is basically considered as the most valuable technology for producing low boiling and high value products by cracking the heavy feed stock such as vacuum residue. The hydrocracking technology plays a key role in modern petroleum refining due to increased product yields and improved product quality meeting both market demand and environmental concerns.

Hydrocracking process normally produces very clean middle distillate fractions with minimum impurities such as sulfur and aromatics. The versatility and flexibility of the process makes it economically attractive to use different types of feedstocks for targeted product slate.

1.4 Steps involved in hydrocracking

1. Preheated feed is mixed with hot hydrogen and allowed to move through a multi-bed reactor with inter stage hydrogen quenches for hydrotreating.
2. Hydrotreated feed is circulated with extra hot hydrogen and moves through a multi-bed reactor with quenches for first pass hydrocracking.

3. Reactor effluents are consolidated and go through high and low pressure separators and are nourished to the fractionator where significant products are drawn from the top, sides and base.
4. Fractionator bottoms might be reused to a second pass hydrocracker for extra transformation as far as possible up to full change.

Table 1.1 Operating conditions involved in hydrocracking process

Parameters	Unit	Value
H ₂ partial pressure	Bar	75-160
Liquid hourly space velocity	hr ⁻¹	0.7-2.5
H ₂ to oil ratio	Nm ³ /m ³	700-800
Nitrogen slip	ppmw	0.1-50+
Conversion per pass		35-80 %

CHAPTER 2

LUMPING METHOD

To accelerate the conversion of the feedstock in the processes, the creation and modification of solid and precise kinetic model is important. Kinetic models are very essential for reactor design, product output and conversion prediction as well as for simulation.

Methods available for kinetic model of heavy oil hydrocracking

2.1 Lumping technique

The modelling criteria used for the cracking of the heavy feed stock uses lumping technique, where components are classified into several chemical families, according to their properties such as molecular weight. This technique simplifies the problem by considering the partition of the species into a few equivalent classes, the so-called lumps or lumping technique, and then assume each class is an independent entity.

The lumping technique is basically classified as,

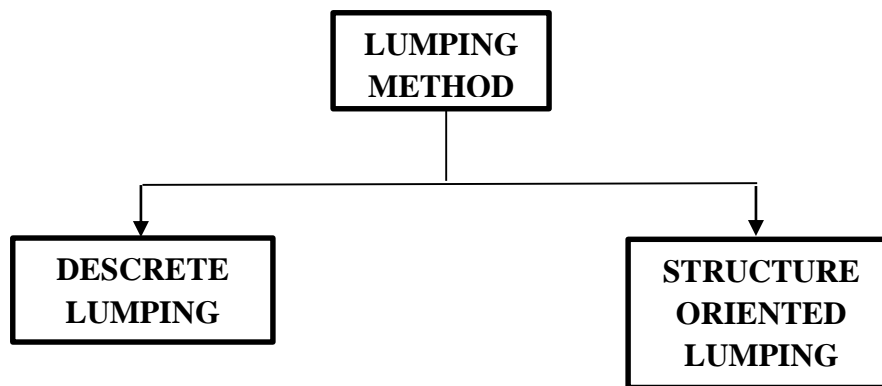
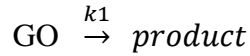


Figure 2.1: Classification of lumping method

2.1.1. Discrete lumping models

The gas oil hydrocracking was studied by Qader and Hill [3], in a continuous fixed-bed tubular flow reactor. The reaction kinetics is of first order with respect to feed concentration and activation energy is of 21.1 kcal/mol.



The reactor output was fractionated into three lumps gasoline, middle distillate and diesel.

Operating conditions:

Temperature: 400–500°C

Pressure: 10.34 MPa

Space velocity: 0.5–3.0 (hr⁻¹)

H₂/oil ratio: 500 Std m³/m³

Callejas and Martí'nez [3] studied the hydrocracking kinetics of Maya crude residue including first-order kinetic scheme. The experiments were carried out in a stirred tank reactor (1 L) in the presence of a NiMo catalyst supported on γ -Al₂O₃.

Number of lumps: AR, atmospheric residuum (343°C+); LO, light oils (343°C-); gases.

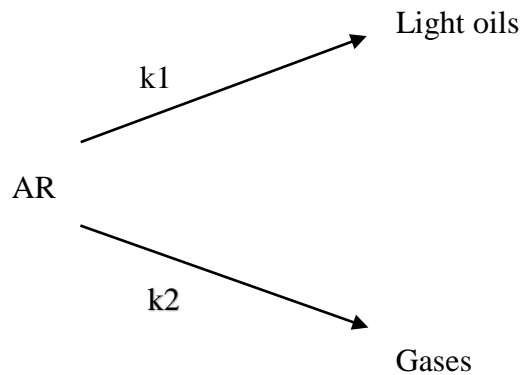


Figure 2.2 : Reaction mechanism

Operating conditions:

Temperature: 375, 400 and 415°C

Pressure: 12.5 MPa

Weight hourly Space velocity: 1.4–7.1 Lgm⁻¹ (cat) h⁻¹

Table 2.1 Rate constants for the hydrocracking of AR

Rate constants (L/gm(cat).h)	375 °C	400 °C	415 °C	E _A (kcal/mol)
k _o (AR conversion)	1.13	3.26	9.20	45.32
k ₁ (light oil formation)	0.07	0.25	1.52	64.40
k ₂ (formation of gases from AR)	0.21	1.5	5.12	70.43

M.A. Callejas, M.T. Martı́nez, Ind. Eng. Chem. Res. 38 (1999) 3285–3289

2.1.2 Structure oriented lumping and single event models

Lumped approach turned out to be very complicated as the heavy hydrocarbon mixture represents large number of groups and reaction pathways. The limitation of lumped models accelerated the development of the kinetic model which are based on molecules. Such models need molecular details of the feed stock. Molecular reconstruction algorithm can be used to develop molecular representation of the feed stock. This algorithm generates a set of molecules from overall petroleum analyses, model hypotheses and chemical knowledge.

Kinetic models based on structure of the molecules involve major part of the data obtained from the modern analytical methods for model reaction modeling at a molecular level, have been highlighted for particular catalytic processes. Lumps are selected for the process under the consideration of the structure of the components present in the mixture.

Liguras and Allen [3] proposed the first method that considers a group of previously defined molecules. Molar fractions of such molecules present in the group were modified so that a mixture having its properties similar to the desired analytical data can be built. They followed a technique that utilizes pure component data in modeling reactions.

Quann and Jaffe [3] showed a method to explain molecules and reactions with a notation of vectors, which permits a program generated in computer to describe the reaction pathways. They constructed a mechanism termed as structure oriented lumping (SOL) to represent vacuum gas oil and lighter fractions. In this lumping method, molecules having same type and amount of structural blocks like structural isomers are explained by the same vector.

Martens and Marin [33] developed a model for the hydrogenated vacuum gas oil hydrocracking. A set of single events was used to describe the reaction mechanism, each of which can be ascribed a rate equation or a term in a single rate equation. The model has included the reaction rules for the carbenium ion which are mainly secondary and tertiary types. The reaction networks were generated by using a computer algorithm.

Such concepts have been preferentially used for particular processes that involve complex reaction mechanism.

CHAPTER 3

LITERATURE REVIEW ON KINETIC MODEL

3.1 Critically involved in modelling for residue conversion

The development of a suitable kinetic model of heavy oil hydrocracking process is not easy due to the complex heavy feedstock used for the process. The analysis of components present in the oil fractions and the complex reaction network of hydrocracking are very difficult. Heavy fractions contain a huge number of hydrocarbons which make the consideration of different compounds and all possible reactions, a hard task. As residue contains not only the molecules consisting of carbon and hydrogen, but also contains hetero atoms such as sulfur and nitrogen and metals like nickel and vanadium.

The development of kinetic models used for refinery feed stocks is not only intricate due to the huge amount of chemical species, reactions and applied rate constants, but its difficulty already begins with the complexity arising in characterization of such feed stock. When a model includes more number of components, more kinetic parameter estimation is required and that increases the necessity of more experimental data.

So various approaches have been mentioned for kinetic modeling of heavy oil hydrocracking.

3.2 Various models existing for residue conversion

Puron et al. (2014) developed a lumped kinetic model for vacuum residue hydrocracking.

Catalyst used: Ni-Mo/Al₂O₃ (aluminum-nickel-molybdenum) and Ni-Mo/Al₂O₃-Cr (alumina doped with chromium).

Ten kinetic models including different reaction pathways among the lumps were generated and solved consecutively. They were developed based on the discrete lumping technique.

Number of lumps: Four lumps (products having boiling point > 450⁰C, products having boiling point < 450⁰C, gas and coke).

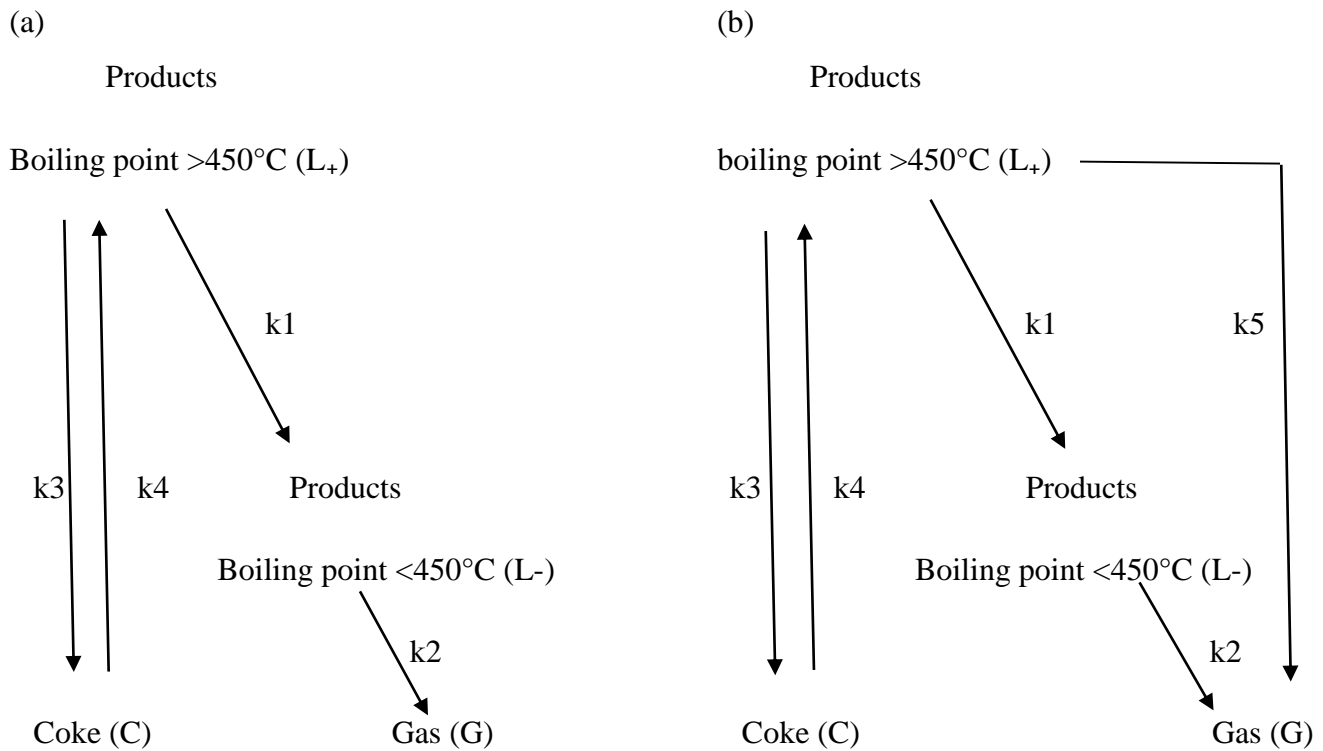


Figure 3.1: Reaction pathways for model 1 (a) and model 10 (b)

Kinetic data were obtained under following conditions:

Feed: 1 gram of the vacuum residue mixed with 250 milligram of the powered catalyst in a micro bomb batch reactor.

Temperature: 400,420 and 450°C

Operating time: 10, 30, 60 and 90 minutes

H₂/hydrocarbon ratio: 5000 scf/bbl

Pressure: 185 bar

The feedstock is completely composed of components having boiling point above 450°C. Each of the reactions among the compounds was considered to be first order.

Model 1 reaction rates are given by equations, which include four kinetic constants.

Products having boiling point $>450^{\circ}\text{C}$: $r_{L+} = -(k_1+k_3)*y_{L+} + k_4*y_c$

Products having boiling point $<450^{\circ}\text{C}$: $r_{L-} = k_1*y_{L+} - k_2*y_{L-}$

Gas: $r_G = k_2*y_{L-}$

Coke: $r_C = k_3 \cdot y_{L+}$

Other models (from 2 to 9) include new reactions along with those involved in model 1. as given in Table 3.1.

Table 3.1 Reactions of the models

Models with all the reactions									
Model	$L_+ \rightarrow L_-$ k1	$L_- \rightarrow G$ k2	$L_+ \rightarrow C$ k3	$C \rightarrow L_+$ k4	$L_+ \rightarrow G$ k5	$C \rightarrow G$ k6	$L_- \rightarrow L_+$ k7	$L_- \rightarrow C$ k8	$C \rightarrow L_-$ k9
1	x	x	x	x					
2	x	x	x	x			x		
3	x	x	x	x	x				
4	x	x	x	x		x			
5	x	x	x	x	x	x			
6	x	x	x	x	x		x		
7	x	x	x	x	x	x	x		
8	x	x	x	x				x	x
9	x	x	x	x	x		x	x	x
10	x	x	x	x	x	x	x	x	x

Note - x indicates that the reaction is included in the model

[4] H.Puron,P.Arcelus-Arrillaga,K.K.Chin,J.L.Pinilla,B.Fidalgo,M.Millan (2013),“Kinetic analysis of vacuum residue hydrocracking in early reaction stage”

The calculations for the Models having different operating conditions were carried out using **Matlab** software with ode45 command to integrate the non-stiff differential equations that explain the kinetic expression for each model.

The lsqnonlin command was used to determine the set of rate constants and optimizing the difference between the model output and the experimental data. lsqnonlin gives the required iterations to obtain the optimum values of the unknown kinetic parameters.

Table 3.2 Kinetic parameters for hydrocracking of vacuum residue (H.Puron *et.al*.,2013)

	NiMo/Al ₂ O ₃				NiMo/Al ₂ O ₃ -Cr			
	Temperature(°c)			E _a (KJ/mol)	Temperature(°c)			E _a (KJ/mol)
	400	425	450		400	425	450	
k(min ⁻¹)	0.0051	0.0102	0.0168	35.7320	0.0050	0.0092	0.0198	41.0274
R ²	0.7913	0.8791	0.8786	0.9964	0.5902	0.8579	0.8576	0.9901

E_a = Activation energy

R² = Linearity coefficients

A first approach in the kinetic analysis was performed taking into account the conversion of VR to products before solving the increasingly more complex ten sequential models. The kinetic constants for the reaction with both catalysts were calculated with the integral method. The activation energies were determined with the Arrhenius equation. The kinetic parameters obtained are reported in table 3.2. The linearity coefficients (R²) obtained for reactions at 425 and 450°C gave values above 0.85, which indicates that a first reaction order reasonably describes the VR conversions obtained for both catalysts.

The results obtained showed that NiMo/Al₂O₃ presented slightly lower activation energy than NiMo/Al₂O₃-Cr, which means that higher conversions and reaction rates must be observed. The model was unable to show some features in the experimental data, for example the larger L₊ conversions obtained with NiMo/Al₂O₃-Cr at the higher temperature. Moreover, it cannot be used to predict product distributions, i.e., relative amounts of L-, C and G, as it only considers one irreversible reaction to all products with an apparent kinetic constant.

Table 3.3 Kinetic parameters obtained from Model 10 (H.Puron *et.al.*, 2013)

Kinetic constants (min ⁻¹)	NiMo/Al ₂ O ₃				NiMo/Al ₂ O ₃ -Cr			
	Temperature (°C)			E _a (KJ/mol)	Temperature (°C)			E _a (KJ/mol)
	400	425	450		400	425	450	
k1	0.0062	0.0144	0.0271	119.47	0.0148	0.0149	0.0531	102.08
k2	0.0044	0.005	0.005	10.46	0.0033	0.0048	0.0048	30.66
k3	0.0731	0.0503	0.0627	n.d.	0.1375	0.0851	0.0295	n.d.
k4	0.504	0.2571	0.273	n.d.	0.814	0.4371	0.0793	n.d.
k5	0.0002	0.0031	0.0112	326.89	0.0003	0.0025	0.0155	319.26
k6	0	0	0	-	0	0	0	-
k7	0.0203	0.0293	0.0491	71.27	0.0816	0.086	0.0985	15.14
k8	0	0	0	-	0	0	0	-
k9	0	0	0	-	0	0	0	-

E_a– Activation energy

n.d. – not defined

Table 3.3 summarizes the values of the kinetic constants of Model10, which were obtained after sequentially solving all the proposed models at the different reaction conditions. The apparent activation energies, calculated by means of Arrhenius equation, are also included. Values for activation energy were not determined when kinetic constants were zero. For the remaining reactions, activation energy values were found to be higher for NiMo/Al₂O₃ than NiMo/Al₂O₃-Cr. As can be seen in table 3.3, k6, k8 and k9 were zero for all the reaction conditions studied. This shows that coke is exclusively produced from L₊ and the reaction pathway towards C formation does not change with temperature. Moreover, it can be concluded that C does not react further to produce L-or G.

According to the values obtained for k2 and k5, the reaction pathway to form G strongly depends on reaction temperature. A slight increase in k2 and a significant increase in k5 are observed when temperature was increased to 425°C. At this temperature, G was produced simultaneously from the cracking of L₊ and L₋. A large increment in k5 was observed when temperature was further increased to 450 °C, while the value of k2 remained constant. This shows that G was produced mainly from cracking of L₊ at 450°C.

k3 takes into account the formation of both types of coke (hard coke and soft coke) and k4 corresponds to the desorption of soft coke into L+. k3 and k4 values for both catalysts decreased when temperature was increased from 400°C to 425°C, showing that coke formation depends on chemical reaction and adsorption on the catalyst. For both catalysts at 400°C, L+ is preferentially converted into L- and C; nevertheless at 425°C the conversion of L+ into G also took place. This pathway shows that when temperature is increased in a batch reactor, coke precursors tend to be thermally cracked, increasing gas formation and decreasing coke formation in the system. On the other hand, for NiMo/Al₂O₃-Cr, increasing temperature from 425 to 450°C leads to a significant decrease in k3 and k4.

An important increase in k1 for NiMo/Al₂O₃-Cr at 450°C was observed. Higher k1 values for NiMo/Al₂O₃-Cr than for NiMo/Al₂O₃ agree with observations from experimental results that the former catalyst remains more active at higher temperatures than the latter. In addition, k5 increased at 450°C, with NiMo/Al₂O₃-Cr having higher values than NiMo/Al₂O₃. Thus, NiMo/Al₂O₃-Cr leads to greater thermal cracking of L+ at 450°C and higher G yields, as observed experimentally.

Hydrocracking of VR over NiMo catalyst is well described with first order kinetics in this work. Lower temperatures leads to the preferential conversion products L+ into L- and coke. Coke is produced exclusively from products >450°C at all temperatures. Gas production was found to depend on the reaction temperature: at lower temperatures it is formed from products <450°C, whereas at higher temperatures gas is predominately produced from products >450°C.

Table 3.4 Yields of VR hydrocracking (H.Puron et,al., 2013)

Time (min)	NiMo/Al ₂ O ₃			NiMo/Al ₂ O ₃ -Cr		
	Temperature (°C)			Temperature (°C)		
	400	425	450	400	425	450
Products >450 °C (L+)						
0	1.000	1.000	1.000	1.000	1.000	1.000
30	0.778	0.631	0.507	0.737	0.641	0.382
90	0.665	0.452	0.271	0.686	0.483	0.206
Products <450 °C (L-)						
0	0.000	0.000	0.000	0.000	0.000	0.000

30	0.090	0.150	0.182	0.110	0.168	0.162
90	0.163	0.201	0.140	0.138	0.205	0.133
Gas (G)						
0	0.000	0.000	0.000	0.000	0.000	0.000
30	0.021	0.081	0.211	0.019	0.067	0.335
90	0.061	0.233	0.490	0.055	0.199	0.551
Coke (C)						
0	0.000	0.000	0.000	0.000	0.000	0.000
30	0.111	0.138	0.100	0.134	0.124	0.121
90	0.111	0.114	0.099	0.121	0.113	0.110

Eduard Manek and Juma Haydary in their paper “Modeling of catalytic hydrocracking and fractionation of refinery vacuum residue” developed a kinetic model.

The kinetic model includes eight reaction steps and six fractions.

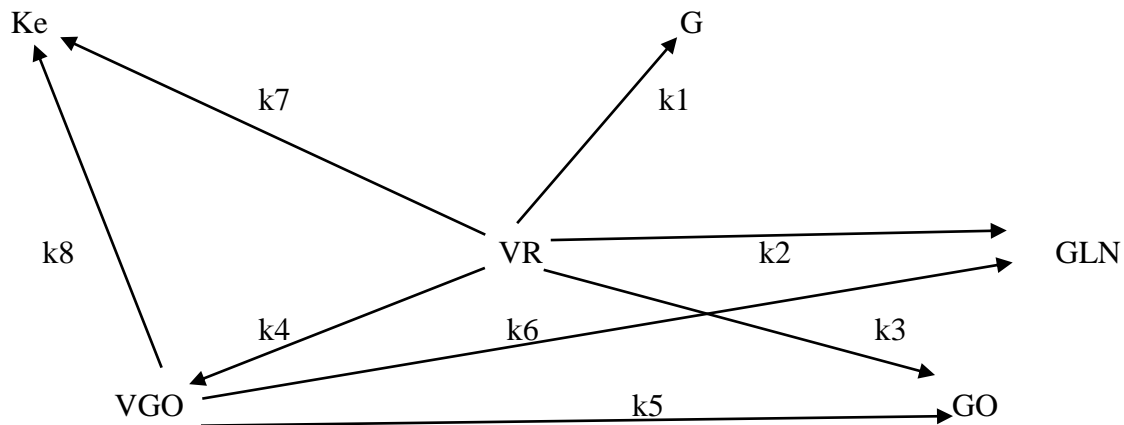


Figure 3.2: Reaction pathways

A commercial catalyst based on Ni–Mo/Al₂O₃ pellets was applied for this process. Temperature in the reactor is generally kept at around 401–412°C and the pressure is held at 18–20 Mpa. First order kinetics was assumed for all pathways:

Kinetic modelling:

The chosen reaction pathways as shown in figure consist of primary vacuum residue (VR) cracking into off gasses (G), naphtha (GLN), kerosene (Ke), gas oil (GO), and vacuum distillates (VGO) and of secondary cracking of vacuum distillates into gasoline, kerosene, and gas oil.

The proposed mathematical model consists of six ordinary differential equations based on the Guldberg–Waage law of mass action: primary cracking of vacuum residue, secondary cracking and production of vacuum distillates from primary cracking, production of gas oil, kerosene, and naphtha fractions from primary and secondary cracking and production of off gasses from primary cracking. Each fraction presented in the equations is expressed as the mass fraction. Kinetic constant as a function of temperature was described by the Arrhenius equation. The independent variables are: residence time (t) and reaction temperature (T). First order kinetics was assumed for all pathways.

Rate equations:

$$d [VR]/dt = -(k_1 + k_2 + k_3 + k_4 + k_7) [VR]$$

$$d [VGO]/dt = k_4 [VR] - (k_5 + k_6 + k_8) [VGO]$$

$$d [GO]/dt = k_3 [VR] + k_5 [VGO]$$

$$d [Ke]/dt = k_7 [VR] + k_8 [VGO]$$

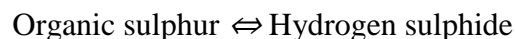
$$d [GLN]/dt = k_2 [VR] + k_6 [VGO]$$

$$d [G]/dt = k_1 [VR]$$

where [VR], [G], [GLN], [Ke], [GO], and [VGO] represent the mass fractions of vacuum residue, off gases, naphtha, kerosene, gas oil, and vacuum distillates, respectively.

Vacuum residue feed contained simple mercaptans (thiols), sulphides, and disulphides. Sulphur from these components was hydrogenated under hydrogen atmosphere into hydrogen sulphide and it was removed in an amine gas treater in the separation section.

In hydrodesulphurisation modelling, all possible reactions are simplified into one reversible process:



The model of hydrodesulphurisation therefore consists of two kinetic equations: organic sulphur removal and formation of hydrogen sulphide. Two Arrhenius equations were used to describe the

hydrogenation pathway (k_S) and the reverse dehydrogenation pathway (k_{S^-}), both with first order kinetics:

$$d[S]/dt = k_{S^-} [H_2S] - k_S [S] \quad \text{and} \quad d[H_2S]/dt = -k_{S^-} [H_2S] + k_S [S]$$

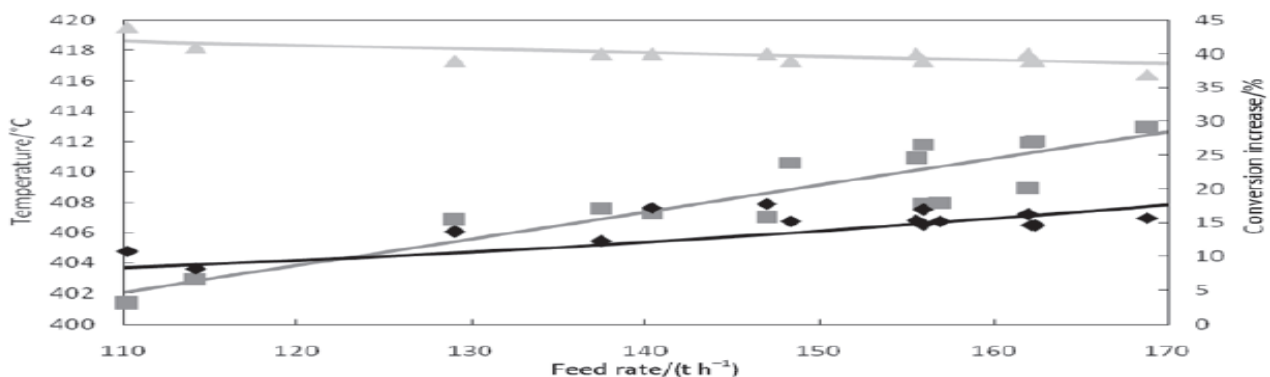
Where $[S]$ and $[H_2S]$ correspond to the amount of organic sulphur and hydrogen sulphide, respectively. Sulphur conversion was measured on daily basis in form of percents of removed sulphur from the feed. The content of sulphur in the vacuum residue feed was around 3.00 mass %.

Simulation of an RHC unit:

The proposed kinetic model allows simulating the current operational status and predicting the new status with different values of the operational parameters. Non-isothermal (temperature profile along the catalyst bed) and isothermal (weighted average bed temperature) conditions were compared by a simulation in terms of the yields. It was found that relative deviation of the mass fractions of each yield of the isothermal and non-isothermal cases is lower than 0.1 %.

In fig3.3, the comparison between the simulated and the obtained data is presented. Deviations of conversions were caused by discrepancies between the experimental and the simulated temperatures. Both simulation and experimental data clearly show that the conversion of VR increases with the increasing feed rate.

As it can be seen from Fig3.2, this statement is not valid for the desulphurization process; higher temperature shifts the equilibrium of the hydrogenation process back. Constant conversion can be ensured by new nonlinear temperature adjustment to the feed rate as shown in Fig2.4. The simulation also shows that to increase the VR conversion from 54 % to 60 %, the temperature increase of approximately 2.7°C is required.



Feed rate vs. feed conversion increase (model —, experimental \blacklozenge), sulphur conversion increase (model —, experimental \blacktriangle), and temperature (model —, experimental \blacksquare) (base line is the current operational status).

Figure 3.3: Comparison of the data

Table 3.5 Comparison of data (Eduard and,Juma ,2014)

Feed Rate (tones/hr)	Temperature (°c)	Feed conversion increase (%)	Sulfur conversion increase (%)
110.5	401.3	11	46
114	403	8	40
129	407	13	38
137.2	407.5	12	39
140.2	407.2	17	39.5
146.8	407	18	39
148.2	410.5	16	37
156	410.7	15	39
156.2	408	17	37
156.3	411.9	14.5	-
157	407.9	15.5	-
161.5	409	16.5	39
162	412	14	38
168.5	412	15	35.5

The kinetic model created in MS Excel was implemented in the Aspen Plus 7.1 program using a user defined model of the reactor (this model allows the input/output of data between Aspen and Excel). The simulation in Aspen Plus starts by generating a set of pseudo-components using the distillation curves of the feed and products. The distillation curve was split into 30 segments; each segment was represented by a specific distillation cut and true boiling point temperature.

For each pseudo-component, also API (American Petroleum Institute) gravity, specific gravity, UOPK (Universal Oil Products k-factor), molar mass, critical pressure, and temperature were calculated. The created set of pseudo-components was exported to MS Excel. The program subroutine determined the reaction kinetics of hydrocracking from the data available for temperature and residence time and a model

of the reaction products distribution into pseudo-components was exported back to Aspen Plus. The reaction products were fractionated in Aspen Plus using the PetroFrac model for atmospheric and vacuum columns. The vapor–liquid equilibrium was calculated by the Broun K10 model.

No distinct relative deviations in the simulation of the isothermal and non-isothermal conditions were found. Temperature has a crucial influence on the product yields. The model can be used to calculate the reaction temperature for given feed rates to obtain the desired conversion at various feed rates.

CHAPTER 4

DEVELOPMENT OF MODEL FOR HYDROCRACKING OF RESIDUE

The model development includes the following steps:

- 4.1 Assumptions for the model.
- 4.2 Reaction pathway involved in the process model.
- 4.3 Reaction equations for the reacting compounds.
- 4.4 Kinetic expression for each of the lumps.
- 4.5 Coding in MATLAB software.

4.1 Model assumptions

1. Hydrocracking reactions occur gradually converting large to small molecules without coke formation.
2. Gas phase is uniform.
3. Liquid phase is also uniform and uniform distribution of the dispersed solid in the liquid phase.
4. First order reactions with respect to reactants.
5. The reactions occur only in the liquid phase and are global reactions between lumps that represent simultaneously the thermal and catalytic contributions.
6. Coke formation mechanism is neglected.
7. No mass transfer of the lumps between the two phases.

4.2 Reaction pathway involved in the model

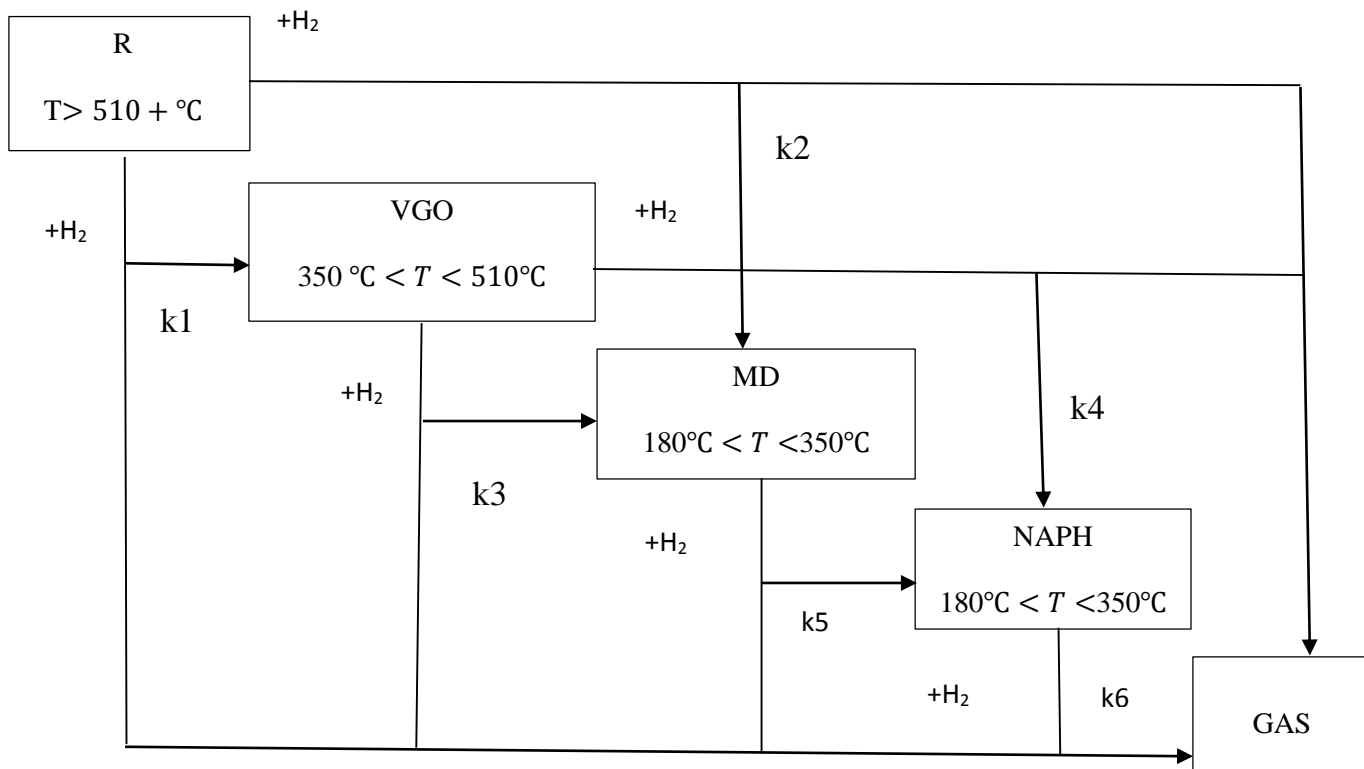


Figure 4.1 kinetic scheme of the hydrocracking of residue

The feed and the liquid products were defined by four boiling point cuts as follows:

Naphtha (NAPH, 40–180°C), distillates (DIST, 180–350°C), VGO (350–510°C), and unconverted residue, (R, 510°C+). Except for hydrogen, the incondensable gases were grouped in the lump named GAS (typically composed of CH₄, C₂H₆, C₃H₈, C₄H₁₀, C₅H₁₂ and H₂S). The global conversion is considered as the conversion of the lump R (C₅₁₀₊ cut) into VGO, DIST, NAPH and GAS lumps (C₅₁₀₋ cut).

4.3 Reaction equations for the reacting compounds

The reaction equations along with the respective rate constants involved in the kinetic model are given below:

1. $R + v_{H_2}^1 H_2 \xrightarrow{k_1} v_{VGO}^1 VGO + v_{GAS}^1 GAS$
2. $R + v_{H_2}^2 H_2 \xrightarrow{k_2} v_{MD}^1 MD + v_{GAS}^2 GAS$
3. $VGO + v_{H_2}^3 H_2 \xrightarrow{k_3} v_{MD}^3 MD + v_{GAS}^3 GAS$
4. $VGO + v_{H_2}^4 H_2 \xrightarrow{k_4} v_{NAPH}^4 NAPH + v_{GAS}^4 GAS$
5. $MD + v_{H_2}^5 H_2 \xrightarrow{k_5} v_{NAPH}^5 NAPH + v_{GAS}^5 GAS$
6. $NAPH + v_{H_2}^6 H_2 \xrightarrow{k_6} v_{VGO}^6 GAS$

4.4 Kinetic expression for each of the lumps

Considering the 1st order rate kinetics, following expressions are taken for the reacting lumps:

$$r_{v,R} = v_R^1 k_1 C_R C_{H_2} + v_R^2 k_2 C_R C_{H_2}$$

$$r_{v,VGO} = v_{VGO}^1 k_1 C_R C_{H_2} + v_{VGO}^3 k_3 C_{VGO} C_{H_2} + v_{VGO}^4 k_4 C_{VGO} C_{H_2}$$

$$r_{v,MD} = v_{MD}^2 k_2 C_R C_{H_2} + v_{MD}^3 k_3 C_{VGO} C_{H_2} + v_{MD}^5 k_5 C_{MD} C_{H_2}$$

$$r_{v,NAPH} = v_{NAPH}^4 k_4 C_{VGO} C_{H_2} + v_{NAPH}^5 k_5 C_{MD} C_{H_2} + v_{NAPH}^6 k_6 C_{NAPH} C_{H_2}$$

$$r_{v,H_2} = v_{H_2}^1 k_1 C_R C_{H_2} + v_{H_2}^2 k_2 C_R C_{H_2} + v_{H_2}^5 k_5 C_{MD} C_{H_2} + v_{H_2}^4 k_4 C_{VGO} C_{H_2} + v_{H_2}^3 k_3 C_{VGO} C_{H_2} + v_{H_2}^6 k_6 C_{NAPH} C_{H_2}$$

$$r_{v,GAS} = v_{GAS}^1 k_1 C_R C_{H_2} + v_{GAS}^2 k_2 C_R C_{H_2} + v_{GAS}^5 k_5 C_{MD} C_{H_2} + v_{GAS}^4 k_4 C_{VGO} C_{H_2} + v_{GAS}^3 k_3 C_{VGO} C_{H_2} + v_{GAS}^6 k_6 C_{NAPH} C_{H_2}$$

Table 4.1 Values of different stoichiometric coefficients

stoichiometric coefficient	value
v_R^1	1
v_R^2	1
v_{VGO}^1	1.6
v_{VGO}^3	1
v_{VGO}^4	1
v_{MD}^2	2.67
v_{MD}^3	1.51
v_{MD}^5	1
v_{NAPH}^4	2.8
v_{NAPH}^5	1.72
v_{NAPH}^6	1
$v_{H_2}^1$	5.84
$v_{H_2}^2$	3.49
$v_{H_2}^3$	4.6
$v_{H_2}^4$	2.08
$v_{H_2}^5$	4.07
$v_{H_2}^6$	1
v_{GAS}^1	.62
v_{GAS}^2	.99

v_{GAS}^3	1.75
v_{GAS}^4	1.45
v_{GAS}^5	.7
v_{GAS}^6	1

At 420°C of operating temperature, k_4 and k_5 becomes zero, which means that VGO to NAPH and NAPH to GAS formation are not happening as the corresponding reactions are not sensitive at the given operating temperature.

On the other hand, at 430°C operating temperature, NAPH to GAS reaction is not sensitive as k_6 becomes zero.

The experimental data and kinetic rate constants in the model are considered based on the range of rate constant value provided by Nguyen *et.al.*, 2013.

Table 4.2 Rate constants at operating temperature of 420 and 430°C

rate constant($m^3mol^{-1}sec^{-1}$)	420°C	430°C
k_1	3729	10105
k_2	9672	20543
k_3	4000	7505
k_4	0	1000
k_5	11066	16747
k_6	0	0

Table 4.3 Molecular weights and densities of the lumps

Temperature	parameters	NAPH	DIST	VGO	R
	density, d_{15}	0.77	0.85	0.93	0.99
430°C	MW	125	227	378	602
420°C	MW	115	212	373	614

4.5 Coding in MATLAB for the kinetic model

In MATLAB software, 'ode15s' solver was considered to solve the system of differential equations. Two different operating conditions of temperature and pressure 420°C and 15.2 Mpa and 430°C and 15.5 Mpa are considered. Initially feed is a mixture of different lumps and initial concentrations are taken at time $t=0$ as mentioned by Nguyen *et.al.*, 2013.

Function file:

```
function dcdt = nguyen_example(t,c)

global k1 k2 k3 k4 k5 k6 c0

%R=cA; VGO=cB; MD=cC; NAPH=cD; H2=cE ;GAS=cF;

cA=c(1); cB=c(2); cC=c(3); cD=c(4); cE=c(5); cF=c(6);

cA0=c0(1); cB0=c0(2); cC0=c0(3); cD0=c0(4); cE0=c0(5); cF0=c0(6);

% reaction kinetics for the model

dcdt(1) = -(k1*c(1)*c(5)+k2*c(1)*c(5));

dcdt(2) = (1.6*k1*c(1)*c(5)-(k3*c(2)*c(5)+k4*c(2)*c(5)));

dcdt(3) = (2.67*k2*c(1)*c(5)+1.51*k3*c(2)*c(5)-k5*c(3)*c(5));

dcdt(4) = (2.8*k4*c(2)*c(5)+1.72*k5*c(3)*c(5)-k6*c(4)*c(5));
```

```
dcdt(5)=(5.84*k1*c(1)*c(5)+3.49*k2*c(1)*c(5)+4.07*k5*c(3)*c(5)+2.08*k4*c(2)*c(5)+4.6*k  
3*c(2)*c(5) +k6*c(4)*c(5));
```

```
dcdt(6)=(.62*k1*c(1)*c(5)+.99*k2*c(1)*c(5)+1.75*k3*c(2)*c(5)+1.45*k4*c(2)*c(5)+.7*k5*c(  
3)*c(5) +k6*c(4)*c(5));
```

```
dcdt = dcdt(:);
```

```
%clear all
```

```
clc
```

```
global T P k1 k2 k3 k4 k5 k6 c0
```

```
%T=(420+273.15);
```

```
T=(430+273.15);
```

```
P=152*105;
```

```
% Specify Initial conditions and other parameters
```

```
cA0 = 590;
```

```
cB0 = 1020;
```

```
cC0 = 645;
```

```
cD0 = 160;
```

```
cE0 = 3300;
```

```
cF0 = 100;
```

```
c0=[cA0 cB0 cC0 cD0 cE0 cF0];
```

```
% k (m3mol-1sec-1) values at 420 degree,
```

```

%k1=3729, k2=9672, k3=4000, k4=0, k5=11066, k6=0;

% k (m^3mol^-1sec^-1) values at 430 degree,

k1=10105, k2=20543, k3=7505, k4=1000, k5=16747, k6=0;

timespan=[0 60];

% Call ODE Solver

options = odeset('RelTol',1e-3,'AbsTol', 1e-6,'Stats','on');

[t , c]= ode15s('nguyen_example',timespan,c0,options,k1,k2,k3,k4,k5,k6);

cA = c(:,1);

cB = c(:,2);

cC = c(:,3);

cD = c(:,4);

cE = c(:,5);

cF = c(:,6);

% Display Results

disp('   time   cA      cB      cC      cD      cE      cF      ')

disp('-----')

disp([t c])

%Plot Results

%plot(t,c,'-')

%ylabel('Concentration')

%xlabel('time')

```

```
%legend('cA','cB','cC','cD','cE','cF')
```

Chapter 5

Result and Discussion

The two different operating conditions of temperature and pressure shows different conversion of feed and production of the lumps.

At 430°C of operating temperature, the conversion of the residue into lighter products is more than compared to that in 420°C of operating temperature. So higher the operating temperature, higher will be the conversion of the feed. The liquid product lumps and GAS production are found to be more at 430°C temperature and 15.5 Mpa of operating pressure. The hydrogen consumption is also high at the higher operating temperature as hydrogen is involved as a reactant in each of the reactions of the lumps.

Table 5.1 Data obtained for the lumps at 420°C

Time(min)	R (mol/m ³)	VGO(mol/m ³)	MD(mol/m ³)	NAPH(mol/m ³)	GAS(mol/m ³)
0	590	1020	645	160	100
30	524.5	1013.4	756.6	277.5	267.9
45	499.5	1009.8	795.5	331.6	338.6
60	478.3	1006.2	827.4	381.4	400.3

Table 5.2 Data obtained for the lumps at 430°C

Time(min)	R (mol/m ³)	VGO(mol/m ³)	MD(mol/m ³)	NAPH(mol/m ³)	GAS(mol/m ³)
0	590	1020	645	160	100
30	463.5	1018.4	861.3	354.5	397
45	425.8	1014.4	920.2	433.9	433.9
60	398.4	1010.1	960	498.8	498.9

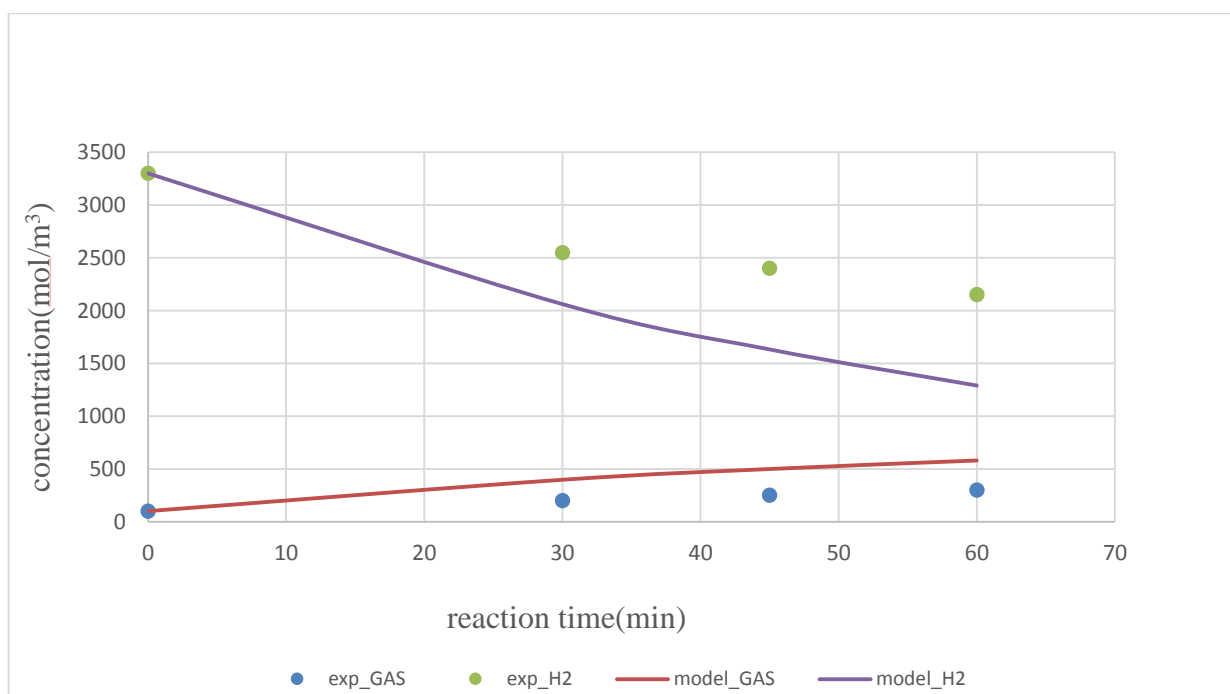
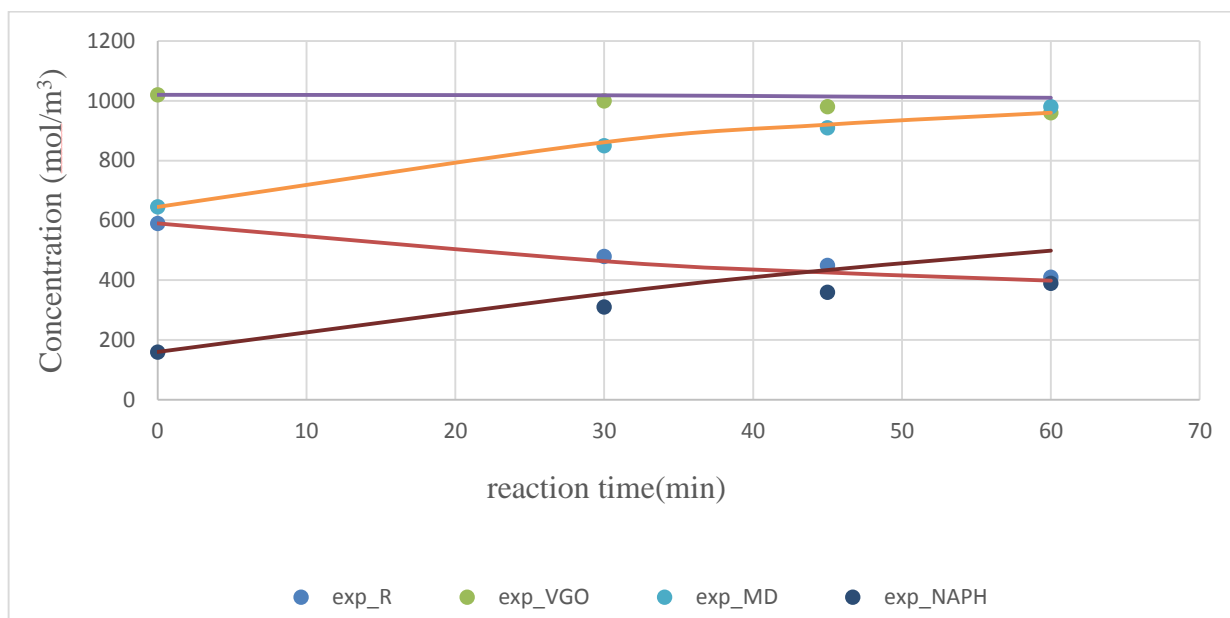


Figure 4.2: Comparison of the model data with experimental data provided by Nguyen *et.al.*, 2013 at 430°C operating temperature

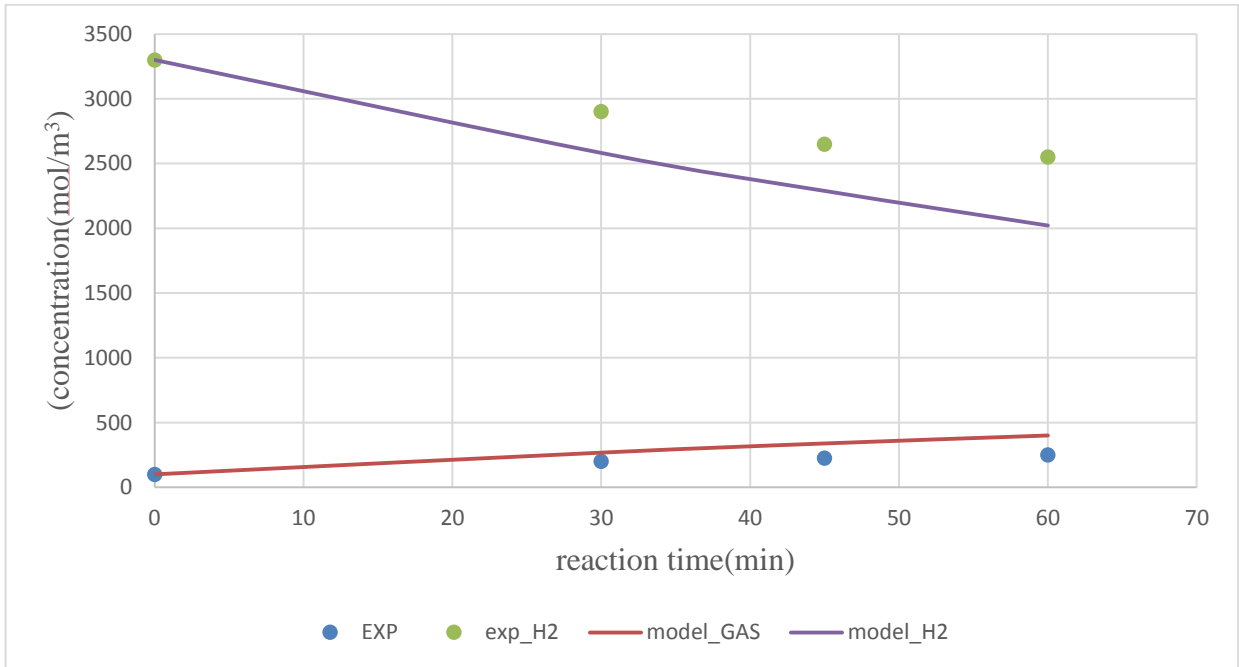
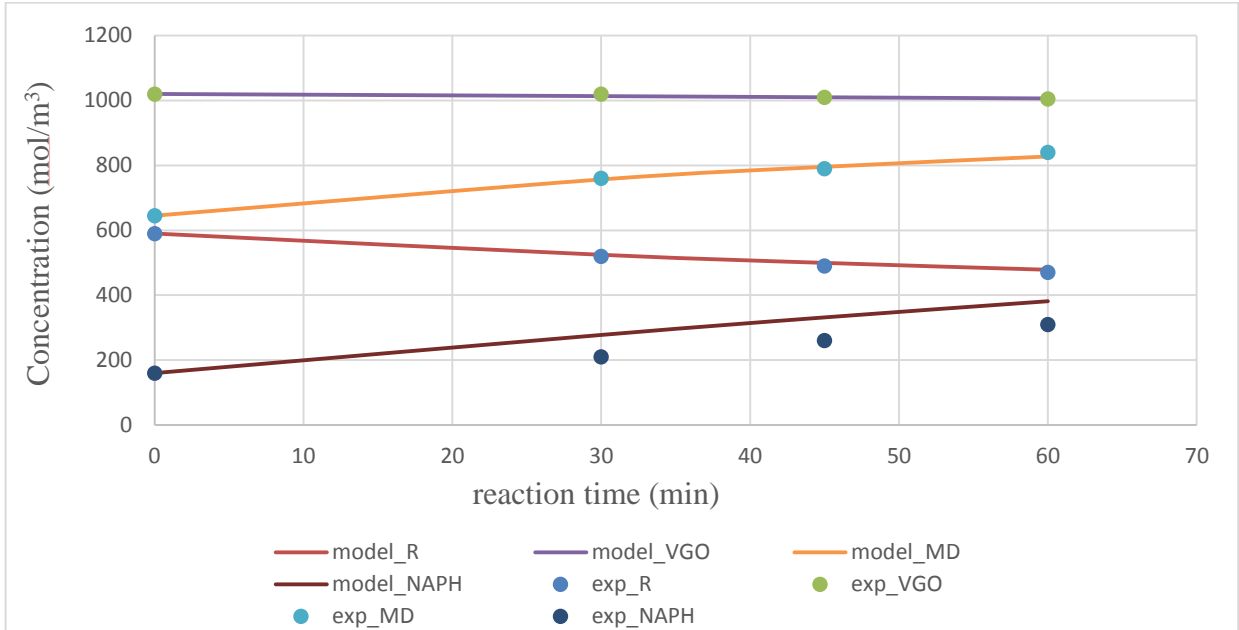


Figure 4.3: Comparison of the model data with experimental data provided by Nguyen *et al.*, 2013 at 420°C operating temperature

CHAPTER 6

CONCLUSION

The model value shows a good agreement with the reported experimental data. The model is only based on kinetics without considering mass transfer between gas and liquid phase.

Future work to be carried out in the model for more accuracy:

1. Incorporation of mass transfer of some lumps in between the two phases.
2. Estimation of the equilibrium compositions of the lumps and equilibrium constant.
3. Development of correlation between the gas and the interface for each of the lumps.
4. Mass balance equations have to be solved by numerical method to estimate the values of the concentrations (C_i^L , C_i^G) at each reaction temperature and time.
5. Finding stoichiometric coefficients and rate constants along with the mass transfer coefficients of the liquid (k_{LA}).
6. Finally comparison of the results with those reported by other authors in literature.

REFERENCES

Alexander Quitian and **Jorge Ancheyta** (2016). Experimental Methods for Developing Kinetic Models for Hydrocracking Reactions with Slurry-Phase Catalyst Using Batch Reactors. *Energy Fuels* 2016, 30, 4419–4437

Blessing Umana, **Nan Zhang** and **Robin Smith** (2016). Development of Vacuum Residue Hydrodesulphurization–Hydrocracking Models and Their Integration with Refinery Hydrogen Networks. *Ind. Eng. Chem. Res.* 2016, 55, 2391–2406

Eduard Manek and **Juma Haydary** (2014), Modeling of catalytic hydrocracking and fractionation of refinery vacuum residue. *Chemical Papers* 68 (12) 1716–1724

H.Puron, **P.Arcelus-Arrillaga**, **K.K.Chin**, **J.L.Pinilla**, **B.Fidalgo** and **M.Millan** (2013). Kinetic analysis of vacuum residue hydrocracking in early reaction stage. *Fuel* 117 (2014) 408–414

Introduction to Hydroprocessing (2016), (Available on: <file:///C:/Users/Windows%208/Desktop/SHEKHAR%20REPORT/INTRODUCTION%20TO%20HYDROPROCESSING%20%20Junaid%20Shah%20%20Pulse%20%20LinkedIn.html>, Accessed on: 12th February, 2017)

Jorge Ancheyta, **Sergio Sanchez**, **Miguel A. Rodriguez** (2005), Kinetic modeling of hydrocracking of heavy oil fractions: A review, *Catalysis Today* 109 (2005) 76–92

Morawski, I; **Mosio-Mosiewski, J** (2006). Effects of parameters in Ni-Mo catalyzed hydrocracking of vacuum residue on composition and quality of obtained products. *Fuel Process. Technol.* 87(7), 659-669.

Thanh SonNguyen, MelazTayakout-Fayolle, MarieRopars, ChristopheGeantet (2013), Hydroconversion of an atmospheric residue with a dispersed catalyst in a batch reactor: Kinetic modeling including vapor–liquid equilibrium. *Chemical Engineering Science* 94,214–223

Tim Jansen, Dimitri Guerry, Emmanuel Leclerc, Marie Ropars, MaximeLacroix, Christophe Geantet and MelazTayakout-Fayolle (2014), Simulation of Petroleum Residue Hydroconversion in a Continuous Pilot Unit Using Batch Reactor Experiments and a Cold Mock-Up. *Ind. Eng. Chem. Res.* 2014, 53, 15852–15861